

University of Massachusetts Amherst  
**ScholarWorks@UMass Amherst**

---

Biology Department Faculty Publication Series

Biology

---

2007

# Measurement of diffusion within the cell wall in living roots of *Arabidopsis thaliana*

EM Kramer

NL Frazer

TI Baskin

Follow this and additional works at: [https://scholarworks.umass.edu/biology\\_faculty\\_pubs](https://scholarworks.umass.edu/biology_faculty_pubs)

 Part of the [Biology Commons](#)

---

## Recommended Citation

Kramer, EM; Frazer, NL; and Baskin, TI, "Measurement of diffusion within the cell wall in living roots of *Arabidopsis thaliana*" (2007). *Journal of Experimental Botany*. 12.  
<https://10.1093/jxb/erm155>

This Article is brought to you for free and open access by the Biology at ScholarWorks@UMass Amherst. It has been accepted for inclusion in Biology Department Faculty Publication Series by an authorized administrator of ScholarWorks@UMass Amherst. For more information, please contact [scholarworks@library.umass.edu](mailto:scholarworks@library.umass.edu).

# Measurement of diffusion within the cell wall in living roots of *Arabidopsis thaliana*

Eric M. Kramer<sup>1,2,\*</sup>, Nicholas L. Frazer<sup>2</sup> and Tobias I. Baskin<sup>1</sup>

1

Biology Department, University of Massachusetts, 611 N. Pleasant St, Amherst, MA 01003, USA

<sup>2</sup> Physics Department, Simon's Rock College, Great Barrington, MA 01230, USA

Received 31 January 2006; Revised 13 May 2007; Accepted 11 June 2007

## Abstract

To quantify the diffusion constant of small molecules in the plant cell wall, fluorescence from carboxyfluorescein (CF) in the intact roots of *Arabidopsis thaliana* was recorded. Roots were immersed in a solution of the fluorescent dye and viewed through a confocal fluorescence microscope. These roots are sufficiently transparent that much of the apoplast can be imaged. The diffusion coefficient,  $D_{cw}$ , of CF in the cell wall was probed using two protocols: fluorescence recovery after photobleaching and fluorescence loss following perfusion with dye-free solution. Diffusion coefficients were obtained from the kinetics of the fluorescent transients and modelling apoplast geometry. Apoplastic diffusion constants varied spatially in the root. In the elongation zone and mature cortex,  $D_{cw}=(3.2\pm 1.4)\times 10^{-11}$  m<sup>2</sup> s<sup>-1</sup>, whereas in mature epidermis,  $D_{cw}=(2.5\pm 0.7)\times 10^{-12}$  m<sup>2</sup> s<sup>-1</sup>, at least an order of magnitude lower. Relative to the diffusion coefficient of CF in water, these represent reductions by approximately 1/15 and 1/195, respectively. The low value for mature epidermis is correlated with a suberin-like permeability barrier that was detected with either autofluorescence or berberine staining. This study provides a quantitative estimate of the permeability of plant cell walls to small organic acids—a class of compounds that includes auxin and other plant hormones. These measurements constrain models of solute transport, and are important for quantitative models of hormone signalling during plant growth and development.

Key words: Apoplast, *Arabidopsis*, carboxyfluorescein, cell wall, diffusion.

## Introduction

Plant growth and development are pervasively influenced by the permeability of the cell wall to ions and small organic molecules. The latter include simple sugars, amino acids, and hormones. While long-distance transport is handled effectively by the vascular tissues of the plant, namely the phloem and xylem, short-distance transport is often mediated in part by diffusion through the cell walls and through the fluid-filled spaces located between cells, a region collectively denoted as the apoplast. The apoplast is a complex, hierarchical material, and transport through it is difficult to predict and little studied quantitatively.

A molecule of particular interest is a major hormone in plants, auxin (indole acetic acid, IAA). Auxin transport is transcellular, that is to say it moves between cells by a process of export across one cell membrane, diffusion through the apoplast, and subsequent import across an adjacent cell membrane. Recently, auxin transport has been the subject of several computational models (Kramer, 2004; Feugier *et al.*, 2005; Swarup *et al.*, 2005; de Reuille *et al.*, 2006; Heisler and Jonsson, 2006; Jonsson *et al.*, 2006; Smith *et al.*, 2006). Most of these models ignore the apoplastic transport step and assume that auxin secreted by one cell immediately enters the adjacent cell (Kramer, 2007). However, a few models have included the apoplast as an explicit compartment and allowed for the possibility that auxin can diffuse relatively large distances (>10 µm) before re-import into a cell. Some model results suggest that diffusion within the apoplast has a notable effect on the distribution of auxin within an organ. Since the magnitude of this effect depends on the permeability of the apoplast to IAA, a quantitative estimate of the diffusion coefficient within the cell wall,  $D_{cw}$ , is needed to refine these models (Kramer, 2006).

\* To whom correspondence should be addressed. E-mail: ekramer@simons-rock.edu

To our knowledge, the diffusion coefficient of auxin has not been measured in the plant apoplast; nevertheless, apoplastic diffusion coefficients have been published for some other small, organic molecules (Richter and Ehwald, 1983; Canny, 1990; Canny and Huang, 1994; Bayliss *et al.*, 1996). These report an enormous range of diffusion coefficients, from  $D/7$  to  $D/1000$ , where  $D$  is the value in water. Because values at the lower end of the range have been ascribed to the presence of a hydrophobic barrier, such as a Casparian strip, that tends to block the diffusion of solutes (Wilson and Peterson, 1983; Schreiber *et al.*, 1999; Hose *et al.*, 2001), the consensus value in the absence of such barriers is of the order of  $D/10$  (Swarup *et al.*, 2005; Heisler and Jonsson, 2006; Kramer, 2006). That  $D_{cw}$  is less than  $D$  is attributable to the steric hindrance posed by cell wall constituents.

Beside the large range of values for apoplastic diffusion, another difficulty for assigning a value to  $D_{cw}$  for IAA is that, among published values for  $D_{cw}$ , there are apparently no data for a carboxylic acid. This is important because IAA is a carboxylic acid, as are abscisic acid, jasmonic acid, and the large family of gibberellins. Within the apoplast, a considerable amount of IAA will be ionized and therefore potentially able to interact with pectins. These polymers have many ionized carboxyl groups that bind calcium, which often cross-links pairs of carboxylic acids (Fry, 1986). Therefore, ionized, acidic ligands diffusing through this pectin network may be slowed by interactions with the fixed calcium ions. Recent results of Proseus and Boyer (2005) hint at such an effect. They injected a solution of fluorescein isothiocyanate (FITC, molecular weight 389 Da, one carboxyl group) into cylindrical *Chara corallina* cell wall ghosts, which are pectin rich. Movement of FITC across the wall from the lumen to the exterior bathing solution was consistent with  $D_{cw}$  being even less than  $D/1000$ .

In this study, the diffusion coefficient of a carboxylic acid was measured in intact *Arabidopsis* roots. The fluorescent dye carboxyfluorescein (CF) was used, CF is an organic molecule chemically similar to auxin and other weak acids. It contains two carboxyl groups, one or both of which are expected to be ionized in the apoplast (see Materials and methods). The dye is taken up by living cells slowly, so that cytoplasmic CF was negligible in the experiments described here. Different perfusion and photobleaching protocols were applied to intact roots immersed in CF solution, and a diffusion coefficient was determined for each case.

## Materials and methods

Seeds of *Arabidopsis thaliana* L Heynh (Columbia accession) were grown on a modified Hoagland's solution (growth medium) under constant light and temperature, as described by Bannigan *et al.* (2006). Seven days after plating, individual seedlings were trans-

ferred to well slides and the portion of the root approximately 5–15 mm from the tip was placed under a coverslip with about 10  $\mu$ l of growth medium. To ensure hydration, the parts of the seedling not under the coverslip were covered with agar growth medium wetted with a few microlitres of growth medium. The well slide was kept covered to decrease evaporation during imaging.

The fluorochrome, 5(6)-carboxyfluorescein (CF) was prepared as a 5 mM stock solution in 10 mM KOH to improve solubility, and stored at  $-20^{\circ}\text{C}$ . An  $\sim 10$   $\mu$ l drop of the CF stock solution was applied to the root along one edge of the coverslip, then excess fluid was blotted from the opposite edge, perfusing CF into the mounting medium. In some experiments, the same perfusion process was subsequently repeated with dye-free growth medium to displace the CF Solution.

To stain for suberin lamellae, berberine was used, modifying the procedure of Brundrett *et al.* (1988). Briefly, intact seedlings were suspended in a solution of 0.5% (w/v) berberine hydrochloride for 10 min, rinsed in distilled water (3 $\times$ 5 min), incubated briefly in 4% (w/v) *n*-propylgallate and 0.1% (w/v)  $\text{FeCl}_3$  to suppress photobleaching, and then mounted in this solution as described above.

Roots were imaged using a Zeiss LSM 510 Meta confocal microscope with 488 nm excitation. Reconstructions from *z*-stacks and other image processing were done with ImageJ 1.36b (NIH, <http://rsb.info.nih.gov/ij/>). Curve fits were done using Kaleidagraph 3.6.4 (Synergy Software, Reading, PA, USA).

The diffusion of CF may depend on its charge. CF has three ionizable groups—a hydroxyl group attached to a tricyclic xanthene and two carboxyl groups attached to an isolated benzene ring (Vallotton and Vogel, 2000). Each of these groups is characterized by its acid–base dissociation constant ( $\text{p}K_a$ ). The commonly cited  $\text{p}K_a$  of CF is for the hydroxyl group ( $\text{p}K_a \sim 6.5$ ) (Bramhall *et al.*, 1987; Vallotton and Vogel, 2000). There are no known published values for the  $\text{p}K_a$ s of the carboxyl groups. However, upper bounds can be placed on these  $\text{p}K_a$ s using the octanol/water partition data of CF provided by Bramhall *et al.* (1987). Curve fits to the partition coefficient as a function of pH give  $\text{p}K_{a1} < 3.8$  and  $\text{p}K_{a2} < 4.3$ . The pH of the Hoagland's medium used in the experiments is weakly buffered near 4.5, the pH of the CF solution used for perfusion is near 5.0, and the apoplastic pH of *Arabidopsis* roots in the region under investigation is generally maintained between 4.8 and 5.5 (Fasano *et al.*, 2001). Thus, the CF in the apoplast is expected to be predominantly in charged forms, with  $< 2\%$  in the neutral form.

To calculate values for  $D_{cw}$ , three anatomical parameters are used: the radial length of an epidermal cell wall,  $L$ , the cross-sectional area of an apoplastic space,  $A$ , and the cell wall thickness,  $h$ .  $A$  and  $L$  were measured in transverse sections from software reconstructions of *z*-stacks.  $L$  fell in the range 8–11  $\mu\text{m}$  and  $A$  in the range 4–10  $\mu\text{m}^2$ . For purposes of error propagation, these are taken as the 95% confidence intervals ( $4\sigma$ ), so  $L = 9.5 \pm 0.8$   $\mu\text{m}$  and  $A = 7.0 \pm 1.5$   $\mu\text{m}^2$ . The cell wall thickness,  $h$  is estimated as  $200 \pm 30$  nm, based on Fig. 9B in Andème-Onzighi *et al.* (2002), where the uncertainty reflects the changes in wall thickness that can result during fixation and sectioning.

## Results

### *Diffusion of CF in water*

To determine the aqueous diffusion coefficient of CF, a small volume of the aqueous CF solution was placed between two coverslips, forming a thin film between 20  $\mu\text{m}$  and 100  $\mu\text{m}$  thick. Under the confocal microscope, a circular spot with a radius of  $\sim 200$   $\mu\text{m}$  and an optical thickness greater than the fluid thickness (to avoid

measurement artefacts due to diffusion in the  $z$ -direction) was bleached. Then the half-time for fluorescence recovery,  $t_{1/2}$ , was determined as the time needed for the intensity at the centre of the disc to reach 50% of the asymptotic recovery value. The exact solution to the diffusion equation, assuming an initial bleached disc of radius  $R$ , gives  $D=R^2/[4\ln(2)t_{1/2}]=0.36R^2/t_{1/2}$  (Crank, 1985). The aqueous diffusion coefficient for CF determined in this way was  $D=(4.87\pm 0.22)\times 10^{-10} \text{ m}^2 \text{ s}^{-1}$  (mean  $\pm$ SE,  $n=4$ ). This value falls in the expected range (Nitsche *et al.*, 2004; Lide, 2006). In the remainder of the paper,  $D=4.87\times 10^{-10} \text{ m}^2 \text{ s}^{-1}$  is used.

### Apoplastic spaces in the root

Living roots were immersed in growth medium containing CF, and fluorescence within the root was imaged by confocal fluorescence microscopy. The optical sectioning capability of confocal microscopy allows images to be obtained at appreciable depths within the *Arabidopsis* root (Fig. 1). In regions of the root outside of the growth zone (henceforth, mature zone), there were prominent spaces at the three-cell junctions between the epidermis and the cortex, and at many of the three-cell junctions between the cortex and endodermis. These spaces were first apparent near the proximal end of the elongation zone, and are clearly visible as longitudinal, CF-bright columns. Using transverse sections reconstructed from confocal  $z$ -stacks (Fig. 1C), it was estimated that the apoplastic spaces have a cross-section area of  $4\text{--}10 \mu\text{m}^2$  (see Materials and methods).

The fluid in each apoplastic space typically appeared to be continuous. Bleaching the CF in a small region within one of these apoplastic spaces usually caused a rapid

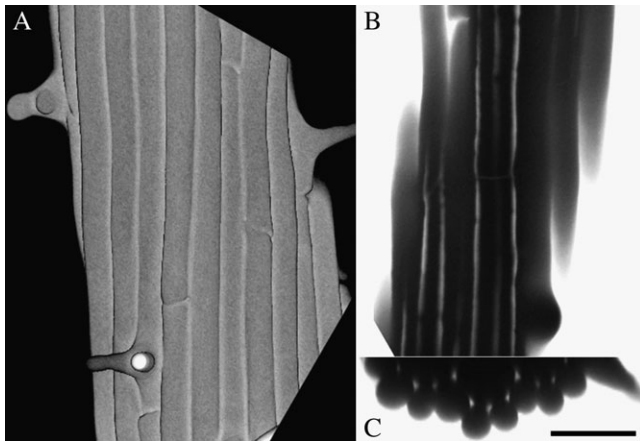


**Fig. 1.** Three views of the same root segment, immersed in CF solution, and imaged on the confocal microscope. (A) Reconstructed images of the root surface, showing epidermal cell files and several root hairs. (B) Optical section through the root tangential to the surface, showing several longitudinal apoplastic spaces filled with CF. (C) Transverse optical section, reconstructed from a  $z$ -series, showing epidermal and cortical cell layers and the CF-filled spaces at three-cell junctions. Scale bar=50  $\mu\text{m}$ .

(<5 s) decrease in brightness over the entire, imaged length (at least 100  $\mu\text{m}$ ) of the space. However, occasionally there was a break in the continuity of the apoplastic space, indicated by a constriction of the fluorescent signal, limiting the movement of bleached CF. Away from these obstructions, the diffusion coefficient of CF in fluid-filled spaces was estimated by measuring the rate of broadening of a bleached profile with time (data not shown). Based on this, the diffusion coefficient of CF within the apoplastic spaces was comparable with, or somewhat smaller than, the aqueous value, although the data have limited accuracy because of the rapidity of the diffusion. Because of the speed of diffusion as well as the intensity of the signal, these spaces were considered to be primarily filled with water. They probably also contain some diffuse pectin, which may have contributed to the smaller diffusion coefficient measured.

### Bleaching one apoplastic space

Several experiments were conducted in which CF in a single apoplastic space was bleached and the entry of unbleached CF into the space was monitored (Fig. 2). The determination of  $D_{\text{cw}}$  based on the recovery kinetics is complicated by the fact that there are two different ways for CF to enter the bleached region: by diffusion from the adjacent cell walls, and by diffusion from the solution within the space adjacent to the bleached zone. A mathematical solution in this case is presented in Appendix 1, with the result that the intensity as a function of time after bleaching is described by:

$$I(t) = c_1 + c_2t - c_3 \frac{\exp(-t/\tau)}{\sqrt{t-t_0}} \quad (1)$$

where the first two terms are a phenomenological fit to the background intensity (i.e. without bleaching),  $t_0$  is the time at the start of fluorescence recovery, and the time constant  $\tau$  characterizes the exchange of CF between the apoplastic space and the three adjacent reservoirs, namely the two neighbouring spaces and the exterior of the root (Fig. 1.1). Note that the third term in Equation 1 would be a simple exponential in the absence of longitudinal diffusion within the space and a simple square root in the absence of apoplastic diffusion. A five-parameter least-squares fit to the measured intensity curves gave  $\tau=44\pm 4 \text{ s}$  ( $n=5$ , mean  $\pm$ SE; Fig. 2).

To obtain a diffusion coefficient from the time constant,  $\tau$ , a solution for this case was derived approximately (Appendix 1, Equation 1.2), giving  $D=LA(3h\tau)^{-1}$ , where  $A$  is the cross-sectional area of the space,  $L$  is the length of the walls separating the space from the adjacent reservoirs, and  $h$  is the cell wall thickness. Substituting  $A=7.0\pm 1.5 \mu\text{m}^2$ ,  $L=9.5\pm 0.8 \mu\text{m}$ , and  $h=200\pm 30 \text{ nm}$  (see Materials and methods), the diffusion coefficient is  $D_{\text{cw}}=(2.5\pm 0.7)\times 10^{-12} \text{ m}^2 \text{ s}^{-1}$  (mean  $\pm$ SD). This

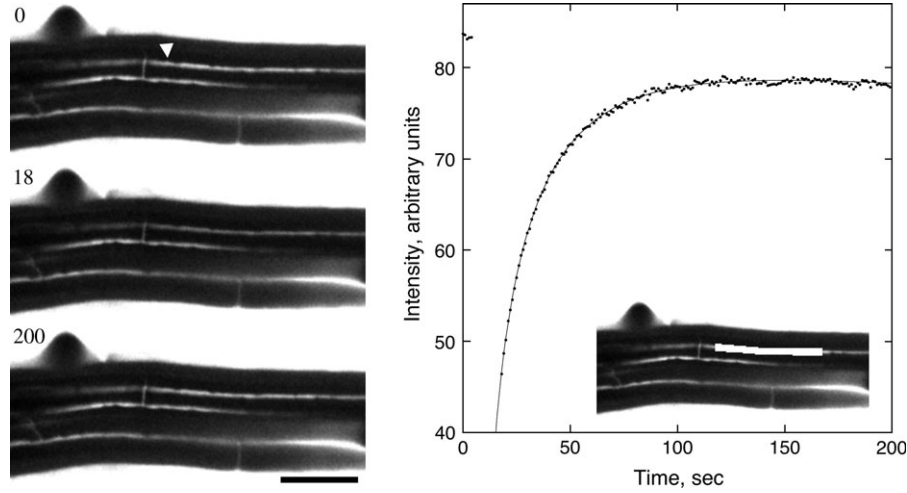


**Fig. 2.** Fluorescence recovery after photobleaching an apoplastic space. Left: three stills from the sequence, showing the root initially, immediately after the bleach, and after recovery. Time in seconds is given at the upper left. The arrowhead indicates the apoplastic space to be bleached. Note that the spaces continue across the entire frame, but appear to end where they pass out of the focal plane. Scale bar=50  $\mu\text{m}$ . Right: mean intensity versus time of the bleached space. Symbols are the measurements; the solid line shows the fit to the data using Equation 1. Bleach interval was from 4 s to 18 s. Inset: the white box shows the region whose intensity was measured.

amounts to a reduction of the aqueous diffusion coefficient by about 1/190.

#### *Perfusion-based recovery*

As an alternative to photobleaching, a dye-saturated root was perfused with dye-free solution and the loss of fluorescence intensity was followed as the CF diffused out of the apoplast (Fig. 3). The apoplastic spaces contain a large volume of CF and hence contribute appreciably to the kinetics of fluorescence decay. Because these spaces are small or absent in the elongation zone, the following treatment considers the elongation and mature zones separately.

#### *Mature zone*

In the mature zone, the total cross-sectional area of the cell walls is small compared with the area occupied by apoplastic spaces. In addition, only a small portion of the cell wall constitutes accessible volume. Thus, the majority of CF will be found in the spaces. For modelling the diffusive loss of fluorescence from the mature zone, only apoplastic spaces were considered. The geometry of the apoplastic reservoir of CF was approximated as shown in Appendix 2, Fig. 2.1. Each trichoblast (root hair-forming epidermal cell) is located at the junction of two cortical cells and separated by two atrichoblasts (non-root hair-forming epidermal cells). The length of all walls is  $L=9.5\pm 0.8 \mu\text{m}$ , as above.

A theoretical treatment of the concentration of CF in the root versus time following a dye-free perfusion is described in Appendix 2. This treatment shows that, at long times, the intensity of the CF in each apoplastic space will decay exponentially,

$$I(t) = c_1 + c_2 t + c_3 \exp(-t/\tau) \quad (2)$$

where the decay constant,  $\tau$ , is the same for each space and the first two terms again allow for gradual changes in the background intensity. The diffusion coefficient in epidermal cell walls is then  $D_{\text{cw}}=2.3 AL(h\tau)^{-1}$  where  $A$  is the mean cross-sectional area of the apoplastic spaces,  $L$  is the radial wall length, and  $h$  is the wall thickness (Equation 2.1). A mean decay time of  $\tau=102\pm 22 \text{ s}$  is found ( $n=6$  roots, mean  $\pm$ SE; Fig. 3A). Substituting the values for  $A$  and  $L$  gives  $D_{\text{cw}}=(7.5\pm 2.0)\times 10^{-12} \text{ m}^2 \text{ s}^{-1}$  (mean  $\pm$ SD). This amounts to a reduction of the aqueous diffusion coefficient by approximately 1/65.

#### *Elongation zone*

In the elongation zone, apoplastic spaces are not conspicuous in the confocal images and presumably have not opened yet. As a result, the simplified geometry depicted in Fig. 2.1 is inapplicable and a mathematical or computer model of the entire root apoplast is needed. An accurate, geometric model is beyond the scope of this paper, but an approximate solution to the perfusion problem is presented in Appendix 3. The wall intensity will decay exponentially, as in the previous section, so the intensity data are again fitted to Equation 2. The relationship between the time constant and the apoplastic diffusion coefficient is  $\tau=(0.6\pm 0.1) R^2/D_{\text{cw}}$ , where  $R$  is the radius of the root (Equation 3.1). A mean decay time of  $\tau=71\pm 11 \text{ s}$  is found ( $n=3$  roots, mean  $\pm$ SE; Fig. 3B). Estimating the radius of the root from confocal images to be  $60 \mu\text{m}$  gave a value of  $D_{\text{cw}}=(3.0\pm 0.7)\times 10^{-11} \text{ m}^2 \text{ s}^{-1}$  (mean  $\pm$ SD) for the elongation zone apoplast. This

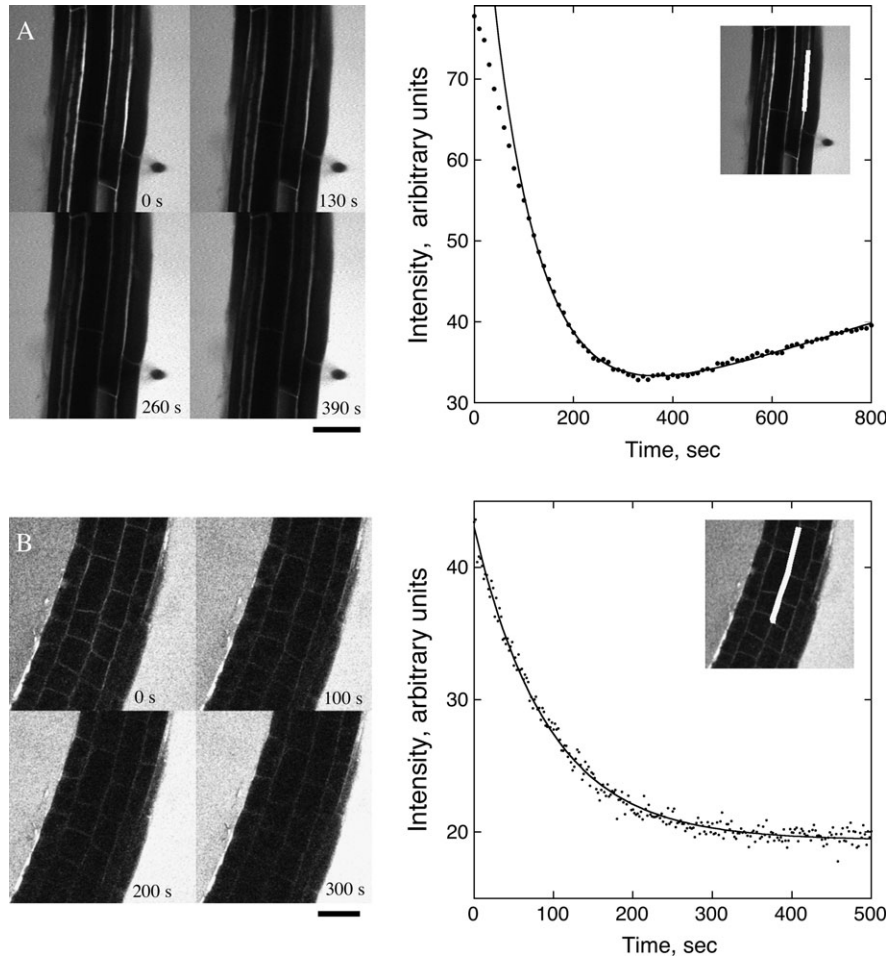


**Fig. 3.** Fluorescence decay following perfusion with dye-free media. (A) Mature zone. Perfusion began approximately 45 s before recording. Left: stills showing the decrease in brightness in the apoplastic spaces. Right: mean intensity versus time of the region shown in the inset (white box is the region measured). Symbols are the measurements; the solid line shows the fit to the data using Equation 2. Intensity during the first  $\sim 100$  s deviates from mono-exponential behaviour. (B) Elongation zone. Perfusion began approximately 45 s before recording. Details as for (A). Intensity of the surrounding fluid increases gradually due to diffusion of CF out of the root. Scale bar=50  $\mu\text{m}$ .

amounts to a reduction of the aqueous diffusion coefficient by approximately 1/16.

#### *Bleaching transverse walls in the mature cortex*

Both previously discussed measures of the diffusion coefficient in the mature zone include epidermal cell walls. As an independent check, the diffusion coefficient was measured in several transverse walls between pairs of cortical cells (Fig. 4). Viewed in a single section, these walls are seen edge-on. Reconstructions based on  $z$ -stacks show that the transverse walls are polygonal, with the longest diameter being about 25  $\mu\text{m}$ . CF-filled apoplastic spaces generally pass through all of the (typically) seven corners, though there was some tendency for the spaces to be constricted near the transverse wall.

To measure the diffusion coefficient, a portion of the wall was bleached and the intensity recovery was monitored. The bleached region was about 12  $\mu\text{m}$  long and

centred at the middle portion of the wall. As shown in Fig. 4, the intensity of the bleached region showed an exponential recovery,

$$I(t) = c_1 - c_2 \exp(-t/\tau) \quad (3)$$

(unlike the perfusion data, there is no need for a term linear in time due to the speed of the recovery). Curve fits gave  $\tau = 3.1 \pm 0.4$  s ( $n=6$ , three roots, two bleaches per root, mean  $\pm$  SE).

To relate the measured time constant,  $\tau$ , to the diffusion coefficient  $D_{\text{cw}}$ , a computer model was made of a bleach conducted on a thin hexagonal wall of uniform thickness (see Appendix 4). Boundary conditions were chosen to mimic CF-filled apoplastic spaces passing through either four or six corners, allowing for the possibility that two spaces were completely blocked at the wall. Spaces of varying diameter, from 0.5  $\mu\text{m}$  to 3.0  $\mu\text{m}$ , were tested, to obtain a range of likely time constants. Simulated bleach

results were similar to real bleaches: the brightness at the centre of the wall showed a short-time behaviour that depended on the bleach geometry, but recovery at longer times was strictly mono-exponential. The relationship between  $\tau$  and  $D_{cw}$  depends on the size and location of the modelled apoplastic spaces, but plausible versions fell in the range  $\tau=(0.17\pm 0.06) L^2/D_{cw}$ , where  $L$  is the long diameter of the hexagon (Equation 4.1). This gave  $D_{cw}=(3.4\pm 1.2)\times 10^{-11} \text{ m}^2 \text{ s}^{-1}$ , which is approximately 1/14 of the aqueous value.

#### Epidermal permeability barrier

The values for the apoplastic diffusion coefficient,  $D_{cw}$ , measured here for CF are summarized in Table 1. All values are smaller than the aqueous value by at least one order of magnitude. In the mature zone, evidence was found for two distinct coefficients. Transverse walls in the mature zone cortex have a diffusion coefficient comparable with that of the longitudinal epidermal walls in the elongation

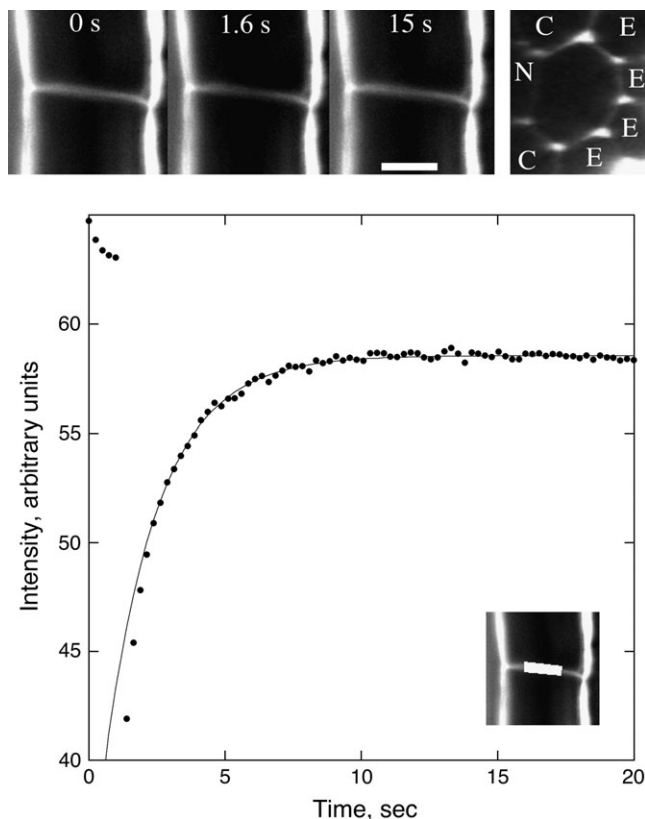


**Fig. 4.** Fluorescence recovery after photobleaching a transverse wall between cortical cells in the mature zone. Top left: three stills from the sequence, showing the root initially, immediately after the bleach, and after recovery. Scale bar=10  $\mu\text{m}$ . Top right: the same wall as seen face-on in a transverse optical section. Adjacent cells belong to the epidermis (E), cortex (C), and endodermis (N). Note that the two apoplastic spaces adjacent to the endodermis appear narrowed or blocked. Bottom: mean intensity versus time of the region shown in the inset. Symbols are the measurements; the solid line shows the fit to the data using Equation 3. Bleach interval was from 1 s to 1.5 s. Intensity during the first  $\sim 2.5$  s deviates from mono-exponential behaviour.

zone; on the other hand, both whole-root perfusions and bleaches of a single, mature zone apoplastic space give a much lower value for diffusion in longitudinal, epidermal walls. These results can be reconciled if the epidermal cell walls have a specifically lowered diffusion coefficient. If so, then the walls of the epidermis would be the primary barrier to the diffusion of CF into and out of the root.

Permeability barriers have been reported previously in the root epidermis, due to hydrophobic molecules chemically similar to those of the Casparian strip (Wilson and Peterson, 1983). To test whether *Arabidopsis* has a similar barrier, a berberine stain commonly used to detect suberin (Brundrett *et al.*, 1988) was applied. As expected, berberine labelled the Casparian strip and suberin lamella of the endodermis, and in addition, cell walls in the mature zone epidermis (Fig. 5A). A second test for suberin-like compounds is autofluorescence under blue or ultraviolet light (Wilson and Peterson, 1983). Using blue (488 nm) excitation, the Casparian strip and suberin lamella of the endodermis of *Arabidopsis* were autofluorescent, while the xylem vessels were not; additionally, the outer walls of mature zone epidermis were autofluorescent (Fig. 5B). Thus, it appears that epidermal cell walls contain a permeability barrier with constituents chemically similar to suberin.

**Table 1.** Summary of measured diffusion coefficients for CF within the cell walls of living *Arabidopsis* roots

$D_{cw}$  data show the mean  $\pm$ SD. Superscripts (a, b, and c) distinguish means whose equivalence is rejected by *t*-test ( $P < 0.05$ ). The last column presents the fold reduction of  $D_{cw}$  compared with  $D$ , the aqueous value.

Protocol	Figure	Tissue	$D_{cw} \times 10^{12} \text{ m}^2 \text{ s}^{-1}$	Fold reduction, $D/D_{cw}$
Bleach	2	Mature epidermis	$2.5 \pm 0.7^a$	195
Perfusion	3A	Mature epidermis	$7.5 \pm 2.0^b$	65
Perfusion	3B	Elongation-zone	$30 \pm 7^c$	16
Bleach	4	Mature cortex	$34 \pm 12^c$	14

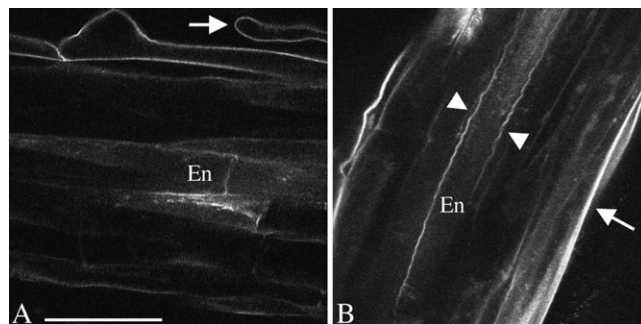


**Fig. 5.** Confocal micrographs indicating hydrophobic cell wall modifications in the mature zone. (A) Berberine staining. Note the stained epidermis, and root hair (arrow). (B) Autofluorescence. The arrow indicates the outer cell wall of the epidermis. Arrowheads indicate the presumptive Casparian strip. En indicates endodermis. Scale bar=50  $\mu\text{m}$ .

## Discussion

As far as is known, the structure and composition of the apoplast of *Arabidopsis* is typical of dicots (Somerville *et al.*, 2004). Advantage was taken of the fact that *Arabidopsis* roots are relatively small and transparent. This allows a confocal microscope to acquire optical sections dozens of microns below the surface of an intact root.

A variety of perfusion and bleaching protocols were applied to probe the diffusion of CF, a charged fluorescent dye, in the apoplast. Taken together, the results show two distinct regimes for diffusion of an organic acid in the *Arabidopsis* root apoplast. In the mature cortex and elongation zone epidermis and cortex, diffusion within the apoplast is of the order of 10-fold slower than in water; whereas, in mature epidermis, diffusion within the apoplast is of the order of 100-fold slower than in water (Table 1). For the mature epidermis, the two estimates for the apoplastic diffusion coefficient are not statistically equivalent, as determined by a *t* test (Table 1). This probably indicates that the assumptions used to derive  $D_{cw}$  from fluorescence measurements are simplistic; for example, it may not be accurate to assume that there are just two permeabilities, one for epidermal cell walls and one for cortical walls. In addition, the larger coefficient measured by the perfusion method may be due to fluid-filled anastomoses connecting the apoplastic spaces with the exterior solution. Regardless of this discrepancy, it is clear that the epidermal cell walls are less permeable than the cortical walls by an order of magnitude. The best measure for the diffusion coefficient of CF in mature epidermis is considered to be the bleach of the apoplastic space, namely  $D_{cw}=(2.5\pm 0.7)\times 10^{-12}$  m<sup>2</sup> s<sup>-1</sup>, and the best measure for the diffusion coefficient of CF in unmodified apoplast is considered to be the mean of the elongation zone and cortex results, namely  $D_{cw}=(3.2\pm 1.4)\times 10^{-11}$  m<sup>2</sup> s<sup>-1</sup>. Expressed as a fraction of the aqueous diffusion coefficient, these are 1/195 and 1/15, respectively.

The reduction in permeability measured in the mature epidermal apoplast is plausibly explained by the presence of hydrophobic molecules that limit diffusion (Fig. 5). An epidermal barrier has been reported previously (Schreiber *et al.*, 1999; Hose *et al.*, 2001). Indeed, Wilson and Peterson (1983) found evidence for wall modifications in the root epidermis of all 27 species they examined. The barrier typically contains suberin, although its composition varies among species, and it typically develops within a few centimetres of the root tip. A detailed study in onion (*Allium cepa*) roots indicated that the modification process starts within 1.5 cm of the root tip, with barrier compounds deposited first in the outermost tangential wall of the epidermis, followed later by deposition in the radial and inner tangential wall (Peterson *et al.*, 1978).

Comparison of the diffusion coefficients reported in Table 1 with those reported previously for the apoplastic diffusion of organic molecules in roots is problematic. Earlier reports have usually been based on the movement of a tracer through an appreciable amount of tissue, with limited ability to distinguish between diffusion through apoplastic spaces, unmodified cell walls, and cell walls with varying degrees of permeability barrier.

Richter and Ehwald (1983) measured the flux of radiolabelled sucrose (molecular weight 342 Da) across discs of parenchyma 2.4 mm thick cut from sugar beet (*Beta vulgaris*) storage tissue. They estimated a value for  $D_{cw}$  between  $D/6$  and  $D/9$  [with the value for  $D$  taken from Lide (2006)]. However, this tissue contains enlarged apoplastic spaces at three-cell junctions (Marry *et al.*, 2006), which are almost certainly filled with fluid rather than air in hydrated tissue. Considering that diffusion through the apoplast is at least an order of magnitude slower than that through water, even a thin film of fluid lining the apoplastic spaces could make a disproportionate contribution to the overall permeability. For example, in the hypothetical case of  $D_{cw}=D/10$ , an aqueous film 100 nm thick could carry the same flux as a wall 1 μm thick. A further complication is that sucrose is taken up actively by sugar beet cells and may have been translocated by cytoplasmic streaming. Thus, the diffusion coefficient in the cell walls of sugar beet parenchyma is probably less than  $D/9$ .

Canny and co-workers studied the penetration of the fluorescent dye, sulphorhodamine G (SG, a zwitterion with molecular weight 533 Da) in roots of several species. Their technique involved the application of SG to the external surface of fresh root segments. In live sections viewed under a coverslip, or in sections frozen and subsequently imaged, they observed the gradual penetration of a fluorescent front and assigned a value for the net apoplastic permeability based on an equivalent homogeneous tissue model (i.e. no distinction between cell walls, spaces, or cells). They found a range of values, depending on species and position within the root tip, ranging from  $D/18$  to  $D/17\ 000$  (Canny and Huang, 1994; Bayliss *et al.*, 1996). They interpreted the lower values as reflecting the development of an epidermal permeability barrier although they did not test for its presence explicitly. Although crude, their results are reasonably consistent with those reported here: unmodified apoplast has a permeability approximately one order of magnitude smaller than the aqueous value, and a hydrophobic barrier can reduce this by at least another order of magnitude.

Finally, Aloni *et al.* (1998) used a protocol in which berberine (an organic cation with molecular weight 336 Da) reacts within the root with thiocyanate to produce a fluorescent precipitate. In sunflower (*Helianthus annuus*), they observed a front of precipitation, moving across the epidermis and advancing into the cortex. While they did



not report a value for the diffusion coefficient, we estimate from their data a value of  $D/10$  for both primary and lateral roots.

Consequently, the present results and others agree that  $D_{cw}$  is at least 10 times smaller than  $D$ . Why should diffusion in the apoplast be slower than in water? One reason is excluded volume: the volume occupied by the molecules that comprise the cell wall decreases the effective cross-sectional area available for diffusion (Grignon and Sentenac, 1991). The excluded volume may include some water molecules that are strongly bound to cell wall polymers, forming a hydration layer inaccessible to a diffusing solute (Dominguez and Heredia, 1999; Mercado *et al.*, 2004). Another reason is steric hindrance: solvent pathways through the wall can be described as a network of pores, and some pores may be too narrow to pass these molecules (Carpita *et al.*, 1979; Baron-Epel *et al.*, 1988). Also, a pore that allows passage may have a tortuous geometry, which increases the path length of diffusing solute molecules (Grignon and Sentenac, 1991). A final reason is due to the large number of fixed negative charges in the cell wall, largely in the form of ionized carboxyl groups. These are expected to repel negatively charged solute molecules, reducing the effective pore diameter. It would be of interest to explore the contributions of these various factors by repeating the present experiments with fluorochromes of different shape, size, and charge.

In the Introduction, it was mentioned that this study was motivated by a desire to quantify the ability of auxin to diffuse through the apoplast. The previous estimate for cell wall permeability,  $D_{cw} \sim D/10$ , was based on published reports using tracers without a carboxyl group, in not very well-defined protocols (reviewed above). The results here confirm that this value is reasonable for carboxylic acids, such as IAA, and refine the previous estimate downward to approximately  $D/15$ . However, the issue of apoplast permeability is complicated: the elongation zone apoplast is homogeneous as far as could be determined, but the mature apoplast has a complex geometry and large spatial variations in permeability.

This technique has not yet been applied to measure the permeability of the Casparian strip. The CF signal in the root endodermis was too faint to allow a localized bleach, like that applied in the cortex, and the perfusion protocol in the mature zone was dominated by the CF in the apoplastic spaces, all of which are exterior to the endodermis. The *Arabidopsis* roots in the present study did not develop an exodermis, which is to say there was no second Casparian strip in the layer of cells just beneath the epidermis (Hose *et al.*, 2001). It may be possible to probe the Casparian strip with a refinement of the technique, for example with two-photon microscopy, which often allows imaging to greater depths. While the Casparian strip is widely regarded as being universally impermeable, there

are some suggestions that the barrier may be permeable to some chemical species, including the protonated form of abscisic acid (Freundl *et al.*, 1998; Hose *et al.*, 2001; Ranathunge *et al.*, 2005).

Apoplastic diffusion of small organic molecules is likely to be important throughout plant development and physiology. Specifically with respect to auxin, apoplastic diffusion constrains the efficiency of transcellular transport and is likely to be important in the regulation of many developmental events (Kramer, 2006). In the mature zone of the root, for example, auxin is a pivotal signal in root hair development. While the fate of epidermal cells to form hair or non-hair cells is determined in the meristem, auxin continues to be required for proper root hair development proximal to the elongation zone (Pitts *et al.*, 1998; Schiefelbein, 2000; Lee and Cho, 2006). As another example, auxin from an emerging lateral root primordium functions as a signal to the cells of the outer root, initiating cell separation and facilitating lateral root emergence (Laskowski *et al.*, 2006; Malcolm Bennett, personal communication). Quantitative models of these processes, among others, will need to incorporate the complexities of diffusion through the apoplast.

## Acknowledgements

This work was supported by the US National Science Foundation, award IBN 0316876 to TIB. The confocal microscopy was accomplished at the Central Microscopy Facility at the University of Massachusetts, Amherst. We thank Alenka Lovy-Wheeler, Alex Bannigan, Dale Callahan, Peter Hepler, David Myers, and Abidur Rahman for invaluable advice and support, and Alex Cobb for a careful reading of the manuscript.

## Appendix 1. Fluorescence recovery after photobleaching one apoplastic space

The simplified geometry used for this analysis is shown in Fig. 1.1. The majority of the apoplastic CF is located in the apoplastic spaces present at each three-cell junction between the cortex and epidermis. Each space has a cross-sectional area  $A$  and an effectively infinite extent parallel to the root axis. Cell walls that separate the spaces from each other and from the exterior fluid all have length  $L$ , thickness  $h$ , and a diffusion coefficient  $D_{cw}$ .

The following approximations were made for the bleach. A longitudinal length  $l$  of one apoplastic space is bleached for a time  $\Delta t$ , then the fluorescence is allowed to recover. In experiments, it was found that the dimming of the signal in apoplastic spaces adjacent to the bleach target was typically small (<20%), indicating that the longitudinal diffusion of CF within those spaces is adequate to keep the concentration of CF approximately time independent during the bleach. This reflects the fact that the diffusion coefficient in the wall,  $D_{cw}$ , is small compared with the diffusion coefficient within the fluid-filled spaces,  $D'$  ( $D' \sim D$ ; see Results). Diffusion in the fluid outside the root is also fast. Thus, as shown in Fig. 1.1, the concentration in the three compartments adjacent to the bleach target was taken to be equal and uniform.

The exact shape of the post-bleach concentration profile in the apoplastic space depends on the duration of the bleach, extinction of

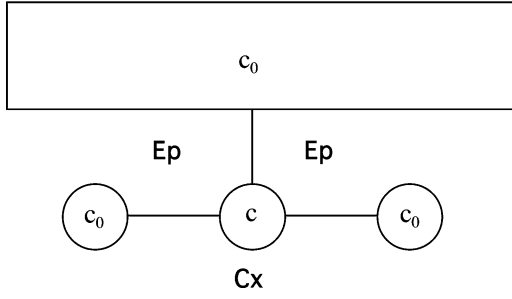


**Fig. 1.1.** Sketch of the apoplastic geometry used in Appendix 1. The large rectangle at the top denotes the exterior fluid with dye concentration  $c_0$ . Smaller circles are three adjacent apoplastic spaces, with the centre one bleached, having concentration  $c$ . Lines connecting fluid reservoirs are cell walls. Ep and Cx denote epidermis and cortex, respectively.

laser intensity inside the root, and the general geometric inhomogeneity of the root cross-section. However, the long-time asymptotic solution in a model apoplastic space is straightforward. Referring to Fig. 1.1, and taking the  $x$ -axis parallel to the root axis, the differential equation for the concentration  $c(x, t)$  is

$$\frac{\partial c}{\partial t} = D \frac{\partial^2 c}{\partial x^2} - \frac{1}{\tau} c \quad (1.1)$$

where  $\tau$  is a time constant characterizing the exchange of CF between the apoplastic space and the three adjacent compartments,

$$\tau = LA(3hD_{cw})^{-1} \quad (1.2)$$

The Green's function for this equation is:

$$G(x, t; x', t') = \frac{\exp[-(t-t')/\tau] \exp\left[-(x-x')^2/2D'(t-t')\right]}{[4\pi D'(t-t')]^{1/2}} \quad (1.3)$$

as can be verified by direct substitution. Thus, at long times ( $t \gg l^2/D' \sim 30$  s) the Gaussian profile will be much broader than the initial bleach length,  $l$ , and the summed intensity in any visible portion of the apoplastic space will vary as:

$$I(t) = c_0 - A \frac{\exp(-t/\tau)}{\sqrt{t-t_0}} \quad (1.4)$$

In practice, it was found to be necessary to add to this expression a term linear in  $t$ , presumably due to slow changes in the concentration of CF in the fluid outside the root. The final form is shown in Equation 1 in the main text. In principle, integrating the Gaussian profile over a finite window in  $x$  ought to provide a quantitative improvement to Equation 1.4 at early times; however, in practice, this led to curve fits that are statistically no better, as judged by the correlation coefficient, and that converge to a reliable fit less often.

## Appendix 2. Time scale for dye loss in the mature zone due to perfusion

It is assumed that the majority of the apoplastic CF is located in the apoplastic spaces present at each three-cell junction between the cortex and epidermis, and between the cortex and endodermis. The geometric approximation, as shown in Fig. 2.1, is similar to that

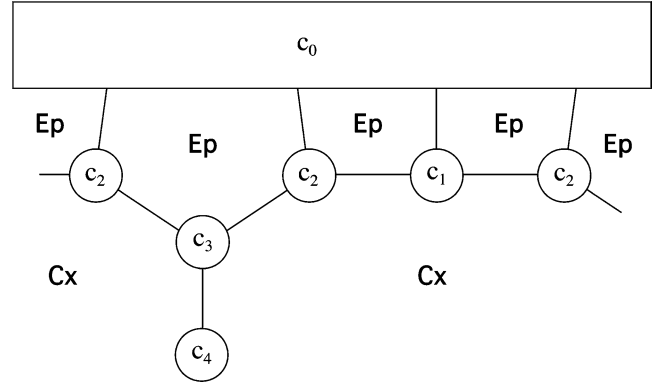


**Fig. 2.1.** Sketch of the apoplastic geometry used in Appendix 2. All symbols are as in Fig. 1.1.

used in Appendix 1. Each compartment has a uniform concentration  $c_i$ . Due to symmetry considerations, there are only four distinct concentrations.

Before time 0, the CF concentration is in diffusive equilibrium with an infinite reservoir outside the epidermis. At time 0, dye-free solution is assumed instantly to replace all exterior fluid, so  $c_0=0$  for all  $t \geq 0$ . Confocal microscopy did not show a significant boundary layer in the exterior fluid. Any boundary layer is expected to be small because apoplastic CF diffuses outward along walls that are about 200 nm thick, but the effective width of the diffusive 'channel' broadens abruptly to the whole width of a cell ( $\sim 10 \mu\text{m}$ ) at the root surface.

Neglecting the small amount of CF within the wall, the following equations describe the diffusive flux of CF (units of  $\text{mol s}^{-1}$ ) from compartment  $i$  to compartment  $j$ ,  $J_{i \rightarrow j} = -D_{cw}lh(c_j - c_i)/L$  where  $l$  is the (arbitrary) longitudinal length of the root segment under consideration and  $h$  is the wall thickness. Referring to Fig. 2.1, the equations for mass conservation are:

$$\begin{aligned} \frac{\partial M_1}{\partial t} &= (Al) \frac{\partial c_1}{\partial t} = 2J_{2 \rightarrow 1} - J_{1 \rightarrow 0} \\ \frac{\partial M_2}{\partial t} &= (Al) \frac{\partial c_2}{\partial t} = J_{3 \rightarrow 2} - J_{2 \rightarrow 0} - J_{2 \rightarrow 1} \\ \frac{\partial M_3}{\partial t} &= (Al) \frac{\partial c_3}{\partial t} = J_{4 \rightarrow 3} - 2J_{3 \rightarrow 2} \\ \frac{\partial M_4}{\partial t} &= (Al) \frac{\partial c_4}{\partial t} = -J_{4 \rightarrow 3} \end{aligned} \quad (2.1)$$

where  $M_i$  is the total mass in a length  $l$  of apoplastic space  $i$ . Assuming all the walls have the same diffusion coefficient  $D_{cw}$ , and substituting  $[c_1(t), c_2(t), c_3(t), c_4(t)] = \exp(-t/\tau)[a_1, a_2, a_3, a_4]$ , four eigenvalues were found for the time constant:  $\tau_1 = 0.197 AL/D_{cw}h$ ,  $\tau_2 = 0.310 AL/D_{cw}h$ ,  $\tau_3 = 0.742 AL/D_{cw}h$ , and  $\tau_4 = 2.75 AL/D_{cw}h$  (using Maple 7.0, here and below). In curve fits to the data, only the longest time scale,  $\tau_4$ , can be reliably measured. Thus the relationship  $D_{cw} = 2.75 AL/h\tau$  is obtained for the mature zone perfusion experiments, assuming that the diffusion coefficient is homogeneous.

As discussed in the main text, the walls between cortical cells probably have a significantly larger diffusion coefficient than the walls surrounding the epidermal cells. The above analysis was thus repeated while assuming that the epidermal cell walls have a diffusion coefficient five times smaller than that of the cortical wall connecting space 4 to space 3 (see Fig. 2.1). This gives a prediction of  $D_{cw} = 2.35 AL/h\tau$  for the epidermal walls and  $D_{cw} = 11.75 AL/h\tau$  for the cortical walls. If the analysis is repeated again assuming the cortical wall has an infinite diffusion coefficient, the predicted epidermal coefficient changes only slightly,  $D_{cw} = 2.28 AL/h\tau$ . Thus

$$D_{cw} = 2.3 AL/h\tau \quad (2.2)$$

If the epidermal walls have a small diffusion coefficient, the perfusion time scale is dominated by the permeability of the epidermal walls and is relatively insensitive to the value for cortex  $D_{cw}$ .

### Appendix 3. Time scale for dye loss in the elongation zone due to perfusion

An exact determination of  $D_{cw}$  would require an accurate map of the elongation zone apoplast and a model for diffusion within it. Barring this, the elongation zone geometry was approximated as follows. Consider a hypothetical longitudinal-radial cell wall that covers the full diameter of the cylindrical root. The wall has diffusion coefficient  $D_{cw}$ , uniform thickness  $h$ , width  $2R$  (where  $R$  is the radius of the root), and effectively infinite extent parallel to the root axis. Before time 0, the CF concentration is in diffusive equilibrium with an infinite reservoir outside the epidermis. At time 0, dye-free solution is assumed instantly to replace all exterior fluid, so  $c_0=0$  for all  $t \geq 0$ . The boundary layer can be ignored for reasons discussed in Appendix 2. The long-time solution for the concentration is  $c(r, t) = A \cos(\pi r/2R) \exp(-t/\tau)$  where  $A$  is an arbitrary constant, and the time constant  $\tau = (4/\pi^2) R^2/D = 0.4053 R^2/D_{cw}$ .

Including the effects of tangential walls will tend to increase the numerical coefficient (i.e. slow down the drainage of CF) by increasing the volume of apoplast to be drained. A more realistic geometry for the wall that includes portions inclined at an angle to the radius will also increase the coefficient by increasing the effective length of the diffusive path. Both effects considered together may increase the coefficient by a factor of  $\sim 2$ . Conversely, including the transverse walls will tend to decrease the numerical coefficient (i.e. speed up drainage) by adding extra pathways for the radial diffusion of CF.  $D_{cw}$  is thus estimated as  $(0.4-0.8) R^2/\tau$ , or, taking the range of 0.4–0.8 as the 95% ( $4\sigma$ ) confidence interval,

$$D_{cw} = (0.6 \pm 0.1) R^2/\tau \quad (3.1)$$

for the elongation zone perfusion experiments.

### Appendix 4. Recovery in a cortical wall

A FORTRAN program, HexDiff, was written that solves the diffusion equation in a hexagonal cortical wall of uniform thickness using an explicit differencing scheme (Press *et al.*, 1989). Boundary conditions were zero flux through the boundary, with the exception of the corners. CF-filled apoplastic spaces were modelled as segments of a disc where the concentration was kept constant at  $c=1.0$  (Fig. 4.1). The diameter of spaces was varied from 0.5  $\mu\text{m}$  to 3.0  $\mu\text{m}$ , reflecting a range of plausible sizes for the spaces. The initial condition was usually a bleached bar along a short diameter with Gaussian brightness profile. Several alternative bleach patterns were tried and it was confirmed that the time constant characterizing the brightness recovery at long times was independent of the shape of the initial bleach. The long-time numerical solution depended on the number and size of the model apoplastic spaces, but always had the form  $I(t) = 1.0 - A \exp(-t/\tau)$ . For model walls with a space at each of the six corners, the time constant ranged from  $\tau = (0.058 \text{ to } 0.15) L^2/D_{cw}$ , where  $L$  is the long diameter of the hexagon, and the smallest coefficient corresponds to the smallest space. For model walls with only four apoplastic spaces (corresponding to the possibility that two adjacent spaces are completely blocked),  $\tau = (0.13-0.28) L^2/D_{cw}$ . Pooling these limits, a reasonable range for the diffusion coefficient as  $D_{cw} = (0.06-0.28) L^2/\tau$ , is arrived at or, taking the range 0.06–0.28 as the 95% ( $4\sigma$ ) confidence interval,

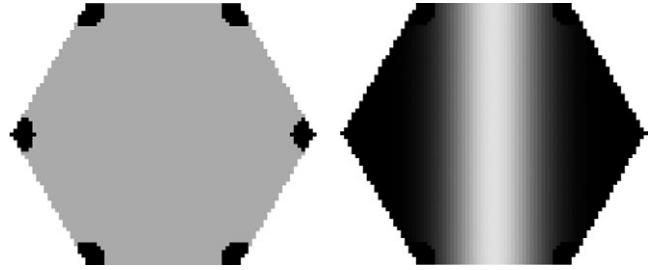


**Fig. 4.1.** Left: hexagonal simulation domain used in the program HexDiff. The concentration at each corner (black) is fixed to a constant value, due to CF in the apoplastic spaces. Right: CF concentration in the domain immediately following a simulated bleach. Black denotes the highest concentration. The laser passes vertically from the top to the bottom of the domain.

$$D_{cw} = (0.17 \pm 0.06) L^2/\tau \quad (4.1)$$

### References

- Aloni R, Enstone DE, Peterson CA. 1998. Indirect evidence for bulk water flow in root cortical cell walls of three dicotyledonous species. *Planta* **207**, 1–7.
- Andème-Onzighi C, Sivaguru M, Judy-March J, Baskin TI, Driouch A. 2002. The reb1-1 mutation of *Arabidopsis* alters the morphology of trichoblasts, the expression of arabinogalactan-proteins and the organization of cortical microtubules. *Planta* **215**, 949–958.
- Bannigan A, Wiedemeier AMD, Williamson RE, Overall RL, Baskin TI. 2006. Cortical microtubule arrays lose uniform alignment between cells and are oryzalin resistant in the *Arabidopsis* mutant, *radially swollen 6*. *Plant and Cell Physiology* **47**, 949–958.
- Baron-Epel O, Gharyal PK, Schindler M. 1988. Pectins as mediators of wall porosity in soybean cells. *Planta* **175**, 389–395.
- Bayliss C, van der Weele C, Canny MJ. 1996. Determination of dye diffusivities in the cell-wall apoplast of roots by a rapid method. *New Phytologist* **134**, 1–4.
- Bramhall J, Hofmann J, DeGruzman R, Montestruque S, Schell R. 1987. Temperature dependence of membrane ion conductance analyzed by using the amphiphilic anion 5/6-carboxyfluorescein. *Biochemistry* **26**, 6330–6340.
- Brundrett MC, Enstone DE, Peterson CA. 1988. A berberine–aniline blue fluorescent staining procedure for suberin, lignin, and callose in plant tissue. *Protoplasma* **146**, 133–142.
- Canny MJ. 1990. Rates of apoplastic diffusion in wheat leaves. *New Phytologist* **116**, 263–268.
- Canny MJ, Huang CX. 1994. Rates of diffusion into roots of maize. *New Phytologist* **126**, 11–19.
- Carpita N, Sabularse D, Montezinos D, Delmer DP. 1979. Determination of the pore size of cell walls of living plant cells. *Science* **205**, 1144–1147.
- Crank J. 1985. *The mathematics of diffusion*, 2nd edn. Oxford: Clarendon Press.
- de Reuille PB, Bohn-Courseau I, Ljung K, Morin H, Carraro N, Godin C, Traas J. 2006. Computer simulations reveal properties of the cell-cell signalling network at the shoot apex in *Arabidopsis*. *Proceedings of the National Academy of Sciences, USA* **103**, 1627–1632.
- Dominguez E, Heredia A. 1999. Water hydration in cutinized cell walls: a physico-chemical analysis. *Biochimica et Biophysica Acta* **1426**, 168–176.

- Fasano J, Swanson S, Blancaflor EB, Dowd P, Kao T-h, Gilroy S.** 2001. Changes in root cap pH are required for the gravity response of the Arabidopsis root. *The Plant Cell* **13**, 907–921.
- Feugier FG, Mochizuki A, Iwasa Y.** 2005. Self-organization of the vascular system in plant leaves: inter-dependent dynamics of auxin flux and carrier proteins. *Journal of Theoretical Biology* **236**, 366–375.
- Freundl E, Steudle E, Hartung W.** 1998. Water uptake by roots of maize and sunflower affects the radial transport of abscisic acid and its concentration in the xylem. *Planta* **207**, 8–19.
- Fry SC.** 1986. Cross-linking of matrix polymers in the growing cell walls of angiosperms. *Annual Review of Plant Physiology* **37**, 165–186.
- Grignon C, Sentenac H.** 1991. pH and ionic conditions in the apoplast. *Annual Review of Plant Physiology and Plant Molecular Biology* **42**, 103–128.
- Heisler MG, Jonsson H.** 2006. Modeling auxin transport and plant development. *Journal of Plant Growth Regulation* **25**, 302–312.
- Hose E, Clarkson DT, Steudle E, Schreiber L, Hartung W.** 2001. The exodermis: a variable apoplastic barrier. *Journal of Experimental Botany* **52**, 2245–2264.
- Jonsson H, Heisler MG, Shapiro BE, Meyerowitz EM, Mjolsness E.** 2006. An auxin-driven polarized transport model for phyllotaxis. *Proceedings of the National Academy of Sciences, USA* **103**, 1633–1638.
- Kramer EM.** 2004. PIN and AUX/LAX proteins: their role in auxin accumulation. *Trends in Plant Science* **9**, 578–582.
- Kramer EM.** 2006. How far can a molecule of weak acid travel in the apoplast or xylem? *Plant Physiology* **141**, 1233–1236.
- Kramer EM.** 2007. Computer models of auxin transport: a review and commentary. *Journal of Experimental Botany* **58**, in press.
- Laskowski M, Biller S, Stanley K, Kajstura T, Prusty R.** 2006. Expression profiling of auxin-treated Arabidopsis roots: toward a molecular analysis of lateral root emergence. *Plant and Cell Physiology* **47**, 788–792.
- Lee SH, Cho H-T.** 2006. PINOID positively regulates auxin efflux in Arabidopsis root hair cells and tobacco cells. *The Plant Cell* **18**, 1604–1616.
- Lide DR, (ed.)** 2006. *CRC handbook of chemistry and physics*, 87th edn. Boca Raton, FL: CRC Press.
- Marry M, Roberts K, Jopson SJ, Huxham IM, Jarvis MC, Corsar J, Robertson E, McCann MC.** 2006. Cell–cell adhesion in fresh sugar-beet root parenchyma requires both pectin esters and calcium cross-links. *Physiologia Plantarum* **126**, 243–256.
- Mercado JA, Matas AJ, Heredia A, Valpuesta V, Quesada MA.** 2004. Changes in the water binding characteristics of the cell walls from transgenic *Nicotiana tabacum* leaves with enhanced levels of peroxidase activity. *Physiologia Plantarum* **122**, 504–512.
- Nitsche JM, Chang H-C, Weber PA, Nicholson BJ.** 2004. A transient diffusion model yields unitary gap junctional permeabilities from images of cell-to-cell fluorescent dye transfer between *Xenopus* oocytes. *Biophysical Journal* **86**, 2058–2077.
- Peterson CA, Peterson RL, Robards AW.** 1978. A correlated histochemical and ultrastructural study of the epidermis and hypodermis of onion roots. *Protoplasma* **96**, 1–21.
- Pitts RJ, Cernac A, Estelle M.** 1998. Auxin and ethylene promote root hair elongation in Arabidopsis. *The Plant Journal* **16**, 553–560.
- Press WH, Flannery BP, Teukolsky SA, Vetterling WT.** 1989. *Numerical recipes*. New York: Cambridge University Press.
- Proseus TE, Boyer JS.** 2005. Turgor pressure moves polysaccharides into growing cell walls of *Chara corallina*. *Annals of Botany* **95**, 967–979.
- Ranathunge K, Steudle E, Lafitte R.** 2005. A new precipitation technique provides evidence for the permeability of Casparian bands to ions in young roots of corn (*Zea mays* L.) and rice (*Oryza sativa* L.). *Plant, Cell and Environment* **28**, 1450–1462.
- Richter E, Ehwald R.** 1983. Apoplastic mobility of sucrose in storage parenchyma of sugar beet. *Physiologia Plantarum* **58**, 263–268.
- Schiefelbein J.** 2000. Constructing a plant cell. The genetic control of root hair development. *Plant Physiology* **124**, 1525–1531.
- Schreiber L, Hartmann K, Skrabs M, Zeier J.** 1999. Apoplastic barriers in roots: chemical composition of endodermal and hypodermal cell walls. *Journal of Experimental Botany* **50**, 1267–1280.
- Smith RS, Guyomarc'h S, Mandel T, Reinhardt D, Kuhlemeier C, Prusinkiewicz P.** 2006. A plausible model of phyllotaxis. *Proceedings of the National Academy of Sciences, USA* **103**, 1301–1306.
- Somerville C, Bauer S, Brininstool G, et al.** 2004. Toward a systems approach to understanding plant cell walls. *Science* **306**, 2206–2211.
- Swarup R, Kramer EM, Perry P, Knox K, Leyser HMO, Haseloff J, Beecher GTS, Bhalerao R, Bennett MJ.** 2005. Root gravitropism requires lateral root cap and epidermal cells for transport and response to a mobile auxin signal. *Nature Cell Biology* **7**, 1057–1065.
- Valotton P, Vogel H.** 2000. Parameter recovery in frequency-domain time-resolved fluorescence spectroscopy: resolution of the prototropic forms of 5-carboxyfluorescein in the physiological pH range. *Journal of Fluorescence* **10**, 325–332.
- Wilson CA, Peterson CA.** 1983. Chemical composition of the epidermal, hypodermal, endodermal and intervening cortical cell walls of various plant roots. *Annals of Botany* **51**, 759–769.